Keeping it Simple – Computational Resources in Deep Generative versus Traditional Methods for Synthetic Tabular Data Generation in Healthcare

Anonymous Full Paper
Submission 21

Abstract

Synthetic data has emerged as a solution to address data access challenges in healthcare, particularly for accelerating AI tool development. Deep generative methods, including generative adversarial networks, variational autoencoders, and diffusion models, have gained prominence for creating realistic and representative synthetic datasets with low re-identification risk. However, while sustainability of future computational needs is a growing topic, computational needs are often overlooked when documenting benchmarking of synthetic data generators.

This study compares computational resources needed using traditional and deep generative methods for generating a synthetic breast cancer dataset, relative to differences in statistical similarity between the training dataset and the synthetic dataset.

The findings reveal that while quality performance within this experiment is comparable, the deep generative methods consume significantly more resources, necessitating High Performance Computing resources. We recommend researchers will increasingly include computational resources as a parameter when benchmarking methods, to build a bigger canvas of literature to guide the method choice.

1 Introduction

There is a growing need for access to high quality data to develop, train or test new AI driven tools ([1]). Synthetic data is seen as a method to overcome the issue of access to sensitive healthcare data ([2]). Some synthetization methods demand high computational resources, making them less available for mainstream use and challenging its future sustainability. Deep generative methods like generative adversarial networks (GANs), variational autoencoders (VAEs) and diffusion models (DMs) have gained traction in the literature as preferred methods to producing high quality synthetic data. With an initial focus on image data, several methods have been tailored to better fit tabular data which is the predominant format for Electronic Health Record (EHR) data.

Although the methods are often reported to create realistic and representative datasets with minimal risk of re-identification, high computational complexity leads to resource requirements concerns ([3]) and should be a consideration for choice of method. Still, for synthetic tabular data in healthcare computational resource needs are rarely addressed in generation method evaluations ([4]).

To guide the practical use of these tools, this study provides an experiment comparing traditional statistical methods and deep generative methods investigating the following questions:

Q1: What are the practical resource requirements for running the pipelines of deep generative methods for generating tabular data compared to traditional generators, and
Q2: How well does deep generative methods perform for generating tabular data compared to traditional generators in terms of statistical similarity?

This experiment benchmarks a traditional method for synthesizing tabular data against deep generative methods, comparing performance in terms of computational resources and statistical similarity to the training data. The experiment on a synthetic breast cancer dataset shows that a traditional generation method – the GaussianCopula - did not require High Performance Computing (HPC) infrastructure yet performed similarly to the resource intensive methods in terms of an average statistical similarity score. This result shows there are situations when the simple methods can be as adequate for the task as the compute heavy methods, making tabular data synthetization available to a broader public in the healthcare sector outside of the academic community.

2 Related Work

Deep generative models seem to be gaining popularity in the literature in the field of tabular healthcare data ([5], [6]). Although it is widely acknowledged that these are more resource intensive than the traditional methods, few have documented the actual difference between the two classes of approaches. [7] point to specific models being developed to fit tabular data like HealthGAN ([8]), MedGAN ([9]), and CTGAN ([10]). A recent review by [4] on synthetic tabular data for healthcare showed that approximately 1/3 of the articles benchmarked deep generative methods against traditional methods like CART ([11]), GaussianCopula ([12]), and Bayesian networks ([13]). Four of these articles mentioned preprocessing needs or computational resources in their evaluation, without necessarily reporting the metrics. None of the articles concluded on computational needs for specific types of generation methods ([4]). There seems to be a need for a greater focus on using sustainable computing or carbon footprint as a performance indicator in the literature.

3 Methods

To compare the performance of the deep generative models on tabular data (Q2), the experiment was run with a GaussianCopula model as a benchmark to the Conditional Tabular Generative Adversarial Network (CTGAN) and Tabular Variational Autoencoder (TVAE). An experiment was run both on a laptop and in a virtual machine (VM) in Microsoft Azure with NVIDIA GPU HPC facilities on the Veracity platform ([14]). The Synthetic Data Vault (SDV) pipeline ([15]) for evaluation metrics for the models were compared to answer Q2, and practical performance measures (size and runtime) was gathered for answering Q1.

3.1 Dataset

The experiment was run using a synthetically generated dataset from the Dutch cancer registry that can be accessed by applying at ([16]), see an extract in Figure A.1 in the Appendix. The dataset is a cohort of 60.000 hypothetical breast cancer patients and has been created with the intention of showcasing what real healthcare data looks like, inheriting both the statistical patterns but also the typical traits of real-world healthcare data like missing values.

Each patient has one row with 47 columns of information about the episode, including measurements of tumor size and location, treatments etc. The table has 60.000 rows x 46 columns (features). Some variables are discrete, and others are continuous. Further details on the data are enclosed in Appendix.

As the dataset has been produced to optimize structural similarity while preserving privacy, this data cannot be expected to be clinically valid and should only be used for methodological experiments. However, the dataset remains useful for comparing the computational requirements of different generators.

3.2 Data preparation

Assuring quality for synthetic data generation starts with the training data [4]. Initial cleaning of the dataset revealed that 10 rows contained missing fields. For the simplicity of this exercise, the rows of patients with missing data were removed. The resulting number of rows left for analysis was 59 990. In a real-life experiment, this may not be an optimal approach as missing data fields is an inherent characteristic of healthcare data and the lack of data may harbor clinical information.

The pipeline was tested both with and without meta data definition. For the meta data definition, it was assumed there is only one tumor per row, even though a patient can have several tumors. This assumption makes both variables patient and episode IDs key-nkr and key-eid primary keys.

3.3 Choice of synthetic data generation models

To simplify the reproducibility of our results and ensure consistency in the implementation of data generators, we opted for using the well-documented ([17]) and maintained open-source python library for synthetic data generation, the SDV library ([15]). The SDV pipeline was chosen as it was the most cited open-source pipeline available at the time of the experiment. This library provides a reliable and standardized framework for synthetic data generation, minimizing the discrepancies that might arise from using different tools or custom implementations. The SDV library's comprehensive documentation and active community support further facilitate the reproducibility and validation of experimental outcomes. Additionally, its origins as a project at MIT lend it academic credibility in the field of synthetic data generation.

A traditional statistical model – the GaussianCopula ([18]) was used to compare the performance of two deep generative models, the TVAE ([19]) and CTGAN ([20]) for the tabular healthcare data.

The GaussianCopulaSynthesizer ([21]) is based on copula functions. A copula in mathematical terms maps the marginal distribution of a variable to the normal distribution through the probability integral transform. This mathematical function allows a description of the joint distribution of multiple variables, analyzing the dependencies between their marginal distributions ([18]).

The TVAE (Tabular Variational Autoencoder) is an adaptation of the variational autoencoder architecture specifically designed for tabular data. It uses an encoder-decoder structure where the encoder compresses the input data into a latent space representation, and the decoder reconstructs the data from this latent space. The TVAE is particularly effective at capturing complex relationships between variables in tabular datasets. The CTGAN (Conditional Tabular Generative Adversarial Network) is a GAN-based model tailored for tabular data. It uses a generator to create synthetic samples and a discriminator to distinguish between real and synthetic data. The ”conditional” aspect allows it to handle both continuous and discrete columns effectively, making it well-suited for heterogeneous tabular data often found in healthcare datasets. Both the TVAE and CTGAN models were presented at the NeurIPS 2019 conference in the paper titled ”Modeling Tabular data using Conditional GAN” ([10]).

3.4 Setting up the infrastructure

The experiments were conducted on two platforms: (1) a Dell laptop with an Intel i7 CPU and embedded Intel GPU (without NVIDIA GPU acceleration), and (2) a virtual machine on the Microsoft Azure-based platform DNV Veracity, equipped with an NVIDIA M60 GPU (including CUDA acceleration). The pipelines for TVAE, CTGAN, and GaussianCopula were deployed on both platforms to compare performance.

3.5 Running the experiment

The original data was split in 20/80. Due to resource consumption, 20 percent (12K patients) were used to train the model while the remaining 80 percent was reserved for evaluating model performance. This split allows us to assess not only how well the synthetic data captures the training data patterns but also how well these patterns generalize to unseen data. On the virtual machine, all three models were trained and tested using two distinct evaluation approaches: (1) unsupervised evaluation (comparing the statistical properties of synthetic data directly with the training data to assess structural similarity); and (2) supervised evaluation (training predictive models on both real and synthetic data, then evaluating their performance on the test set to assess the utility of the synthetic data).

The training was done first without defining meta data – describing whether a column (feature) is numerical or categorical. An additional test was done using only TVAE and the GaussianCopula after manually defining this meta data, to evaluate the effect. To facilitate the reproducibility of our experiments, we used the default hyperparameters as defined in the source code for the corresponding generators ([22], [23], [24]).

For the laptop experiment, a smaller amount of training data was used (10 percent of the data). The deep generative models were trained and tested to explore resource consumption. The CTGAN had to be aborted due to resource overload.

3.6 Quality evaluation

Our evaluation framework employed both unsupervised and supervised approaches to comprehensively assess synthetic data quality. The SDV Evaluation Metrics Library from the original Synthetic Data Vault Project ([15]) was used to evaluate the synthetic data generated from each model. The evaluation included SDV’s quality report and diagnostics report. The quality report ([25]) presented weighted scores on column shapes and column pair trends. The column pair trends describe structural similarity between the synthetic data and the test data; how they vary in relation to each other, for example the correlation. The higher the score, the more the trends are alike ([15]).

The diagnostic report ([26]) presented two similarity scores that compare synthetic data with the test data, and one score on privacy risk: coverage and boundaries (similarity) and overfitting/copying of test data (privacy risk) ([27]).

Coverage means how well the synthetic data covers the categories present in the real data. Boundaries is a measure of how well the synthetic data follows the min/max boundaries set by the real data. The score is between 0 and 1, and the higher the score the better. Overfitting is evaluated by a measure of how many rows are copies of the original data.

Using an automated pipeline for quality evaluation is easy to implement and use but may not show all quality dimensions that should be investigated if the synthetic data is to be used in a safety critical clinical context ([4]). While average scores are practial for benchmarks, they can obscure deviating performance for specific features, and diagnostic exercises was performed to evaluate featurewise similarity in addition to the scores. In this pipeline, there was no bias or fairness metrics, no clinical usability, and only one privacy measure. For the context of this experiment, this was deemed sufficient.

4 Results

There were significant differences in the resource needs for running the generation pipelines, and only minor differences in the measured average statistical similarity between the generators.

The computational needs for the generative methods were significantly higher than the traditional method, to the point where certain parts of the experiment were not feasible to complete. When meta data was defined, the GaussianCopula outperformed the two other models in all similarity scores. When meta data was not defined, the performance of GaussianCopula dropped to below that of the deep generative method TVAE, the TVAE performance was more robust to the lack of meta data.

The results section is divided into answering the

Table 1. Practical performance of the different models, training time and model size. Only the experiment without meta data was run on the laptop.
** The CTGAN laptop experiment was manually aborted.*
*** The CTGAN HPC experiment without meta data was not completed due to CUDA out of memory errors.*

Generation method	Time laptop	Time Azure	Model size
WITHOUT META DATA			
GaussianCopula	NA	17 sec	1.5 Mb
CTGAN	more than 420.000 sec*	NA**	7825 Mb
TVAE	54.000 sec	1200 sec	7.5 Mb
WITH META DATA			
GaussianCopula	NA	4 sec	0.5 Mb
CTGAN	NA	480 sec	33 Mb
TVAE	NA	120 sec	0.5 Mb

two questions, respectively.

4.1 Pipeline requirements for processing capacity (Q1)

The models were trained on 20 percent of the cleaned original dataset (11.998 records) on the virtual machine, both with and without defining meta data (numerical vs categorical values). Table 1 shows results of training time and storage needs for the models. The training time was notably shorter for the traditional GaussianCopula model compared to the deep generative models with a factor ranging from 30 to 565 times faster. Without defined meta data, and running on the azure server, the traditional GaussianCopula model used 17 seconds and the TVAE used 1200 seconds. Notably, the CTGAN evaluation in the ”without meta data” scenario could not be completed due to CUDA out of memory errors on our GPU setup, highlighting the substantial memory requirements of this model when processing unstructured data. With meta data the training was faster for all models, rendering the relative differences smaller but with a similar distribution. Storage was notably smaller when the meta data was defined.

The laptop setup proved impractical for the deep generative methods. While the TVAE generator could run, it took an excessively long time. The CTGAN was stopped after two days due to its prolonged runtime. These results highlight the necessity of High Performance Computing (HPC) resources for deep generative methods when working with tabular data of this scale.

4.2 Similarity benchmark of generator performance on tabular data (Q2)

Table 2 shows results from the similarity evaluation on the synthetic data run on models with and without defined meta data (as detailed in meta data schema of SDV developer guide 13). With meta data, the TVAE performs adequately but not as well as the simple statistical approach (GaussianCopula) on the tabular data, with slightly lower scores for column shapes, column pair trends and coverage. The TVAE shows slightly lower quality scores than the CTGAN and lower coverage. The table values for metrics in the experiment with manually defined meta data have four digits to emphasize the difference between CTGAN and TVAE.

Table 2. Quality evaluation scores of the models run with and without manually defined meta data. Scores are between 0 and 1, higher score is better quality. Description of the quality parameters in section 3.6. Quality evaluation and details can be found in the [15] library. (See larger version and data labels dictionary in appendix.)
*** The CTGAN HPC experiment without meta data was not completed due to CUDA out of memory errors.*

Metrics	GaussianCopula	CTGAN	TVAE
WITH META DATA			
Quality score			
Column shapes	0.9247	0.8831	0.8813
Column pair trends	0.8711	0.8211	0.8158
Diagnostics			
Coverage	0.97	1.0	0.93
Copies	1.0	1.0	1.0
Boundaries	1.0	1.0	1.0
WITHOUT META DATA			
Quality score			
Column shapes	0.76	NA**	0.81
Column pair trends	0.61	NA**	0.72
Diagnostics			
Coverage	0.92	NA**	0.76
Copies	1.0	NA**	1.0
Boundaries	1.0	NA**	1.0

Analysing the coverage pr feature, the column shapes showed a more consistent performance with the GaussianCopula with the average score of 0.97 versus the TVAE average score of 0.93. The graphs for column coverage (see figure 1) show a difference in the performance for numerical versus (dark blue columns) categorical values (light blue columns). The TVAE performs better than the GaussianCopula on numerical values, while the GaussianCopula performs better for the categorical values. The same trend was seen on column shapes.

The TVAE performed noticeably worse for one specific variable (tumor morphology). The distribution of this variable was quite particular and difficult to capture for a generator, with ductal carcinoma (code 8500) being noticeably larger than the other groups with 44.426 instances, Lobular carcinoma (code 8520) with 7245 instances and the residual 28 groups having a count below 1000 instances (224-889 instances). The distribution of the original data for this feature is shown in Figure A.4.

When meta data was not manually defined, the TVAE showed better overall similarity performance scores than the GaussianCopula, showcasing the potential of deep generative models compared to tra-

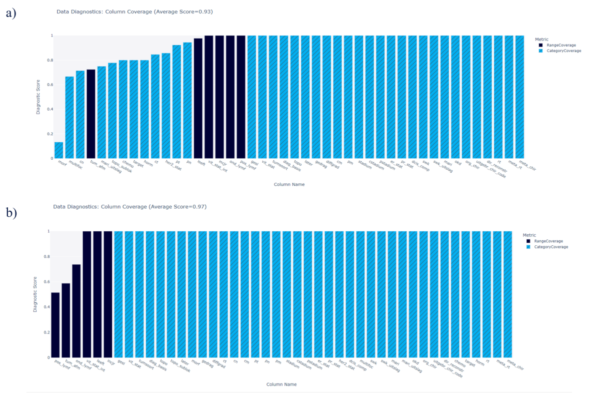

Figure 1. The figure shows a detailing of the average column coverage score provided in Table 2 in the experiment when the meta data was defined, comparing a) the TVAE results and b) the GaussianCopula results. The dark blue RangeCoverage is used for numerical values and the light blue CategoryCoverage is for categorical data. See the appendix for a bigger version of the image.

ditional models, for learning the underlying patterns of a dataset.

5 Discussion

All pipelines were faster when meta data was manually defined. The statistical GaussianCopula pipeline was the fastest and smallest in terms of storage need. When it is necessary to work with the computationally demanding deep generative pipelines, it could be beneficial to use the statistical model to iterate on your experiments and see that your meta data is correct before running the more time-consuming generators. It was possible but not practical to run the TVAE generator on a laptop since the size of the seed dataset had to be limited and it had an impractically long runtime (15 hours). The resource needs for the CTGAN in this experiment confirms the potential extent of computational requirements for tabular data generation with deep generative models, even in the HPC setting. For the community to move forward in a sustainable way, it would be beneficial to choose traditional and less compute intensive methods when quality needs and performance requirements allow it.

When choosing a generation method, one should consider all relevant quality dimensions– similarity, usability (clinical and other), privacy, bias and fairness and carbon footprint ([4]) and prioritize them according to the intended downstream use of the dataset. While investigating all perspectives is particularly important in potential high-impact areas like healthcare, fairness was excluded in this experiment due to the dataset composition (one gender and homogeneous population, lacking minority groups).

The Gaussian Copula had the highest average quality score when meta data was defined, while the TVAE showed better consistency in performance independently of predefined meta data. The detailed findings of the column coverage (figure 1) shows that for certain parameters (tumor morphology) the TVAE showed poor column coverage. This can be explained by the disproportionate distribution of this variable in the training data. Gaussian Copula seemed to perform noticeably worse on numerical data compared to the TVAE, but as there were few numerical values in the dataset this did not affect the average scores significantly.

An average score such as the SDV quality evaluation score used in this paper is useful for benchmarking generators on a generic level, but in choosing the relevant quality parameters for a specific clinical case, one must consider the cohort and what clinical desiderata are relevant for these according to the intended use.

A conclusion on quality performance and choice of an optimal generation model cannot be generic and must always be adjusted to the specific data and clinical case at hand.

Limitations This paper is a synthetic experiment with no downstream use, and therefore no considerations for specific parameters have been discussed. The training dataset used in the experiment is a synthetically generated dataset. Since the real data is not accessible, the actual objective quality compared to reality cannot be determined. Creating a synthetic dataset based on a synthetic dataset can only be seen as a practical or methodological test. An important limitation of this study is the reliance on a single library (SDV) for implementation of the synthetic data generation models. While SDV is well-documented and widely cited, using a single library may limit the generalizability of our findings. Future studies should consider implementing models using multiple libraries to provide a more comprehensive comparison. There are also other open libraries available like the recently published SynthCity at Cambridge ([28]), and new evaluation metrics are being proposed in the literature. The SDV pipeline could preferably be expanded by additional quality metrics ([29]). In the experiment, we relied on two out-of-the-box reports natively provided by the SDV library: ”The Diagnostic Report” and ”The Quality Report”. According to the library developers, these two reports provide scores for an aggregated and overall comparison of original and synthetic datasets. While this approach offers a simplified version of reporting, focusing on computational resources and their comparisons, we acknowledge that it lacks more rigorous statistical testing. In the experiment, the standard SDV pipeline metrics were used as these are perceived as commonly used for statistical similarity. It is unclear whether this score properly rewards the desired model behaviour, resulting in uncertainty around the results. The evaluation metrics used in this case will not evaluate the usability of the data and the clinical logic like the realism of the TNM classification of tumors in the different cases or in downstream performance. Fairness metrics are not included, and only a simple similarity metric of statistical closeness is used for measuring privacy. The study is limited to only three generation methods. In the future, we plan to investigate newer and potentially more effective models such as diffusion and large language models.

To conclude on the actual clinical utility of the synthetic data produced by the pipelines, this experiment should be recreated on a real dataset and for a defined downstream application. Other quality metrics and mechanisms should also be added, to evaluate the clinical usability and logic of the resulting synthetic data.

To better guide practitioners in making sustainable choices, computational resources should be included as a reporting parameter for benchmarking of methods. To ensure a focus on sustainable computing, metrics of training time and model size could be translated into a more comparable metric like carbon footprint.

Further work This experiment covers one data modality - tabular data - with synthetic national cancer registry type data on breast cancer, and using two deep generative methods and one traditional method. The generators used were considered most common at the time of the experiment and available in a public pipeline. To investigate the robustness of the conclusions, there is a need for a wide range of benchmarks on a range of different datasets, investigating other types of both deep and traditional generators and for differing use cases and data modalities, including more thorough hyperparameter exploration. Future studies could consider implementing models from multiple libraries to provide a more comprehensive comparison. For instance, the recently published SynthCity library developed at Cambridge University ([28]) could be used alongside SDV to broaden the scope of the analysis and validate findings across different implementations. In addition, future research should investigate the differences in quality scores for a broader range of evaluation criteria covering topics like fairness, privacy and other representativity (similarity and usability) metrics.

6 Data availability

The synthetic data from the Dutch breast-cancer cohort is available at the website of the Cancer Registry of Netherland ([16]).

References

[1] R. J. Chen, M. Y. Lu, T. Y. Chen, D. F. Williamson, and F. Mahmood. “Synthetic data in machine learning for medicine and healthcare”. In: *Nature Biomedical Engineering* 5.6 (2021), pp. 493–497.

[2] M. Giuffrè and D. L. Shung. “Harnessing the power of synthetic data in healthcare: innovation, application, and privacy”. In: *NPJ Digital Medicine* 6.1 (2023), p. 186.

[3] L. Lannelongue, J. Grealey, A. Bateman, and M. Inouye. *Ten simple rules to make your computing more environmentally sustainable.* 2021.

[4] V. B. Vallevik, A. Babic, S. E. Marshall, S. Elvatun, H. M. Brøgger, S. Alagaratnam, B. Edwin, N. R. Veeraragavan, A. K. Befring, and J. F. Nygård. “Can I trust my fake data – A comprehensive quality assessment framework for synthetic tabular data in healthcare”. In: *International Journal of Medical Informatics* 185.May 2024 (2024).

[5] H. Murtaza, M. Ahmed, N. F. Khan, G. Murtaza, S. Zafar, and A. Bano. “Synthetic data generation: State of the art in health care domain”. In: *Computer Science Review* 48 (2023), p. 100546.

[6] A. Gonzales, G. Guruswamy, and S. R. Smith. “Synthetic data in health care: A narrative review”. In: *PLOS Digital Health* 2.1 (2023), e0000082.

[7] M. Hernandez, G. Epelde, A. Alberdi, R. Cilla, and D. Rankin. “Synthetic data generation for tabular health records: A systematic review”. In: *Neurocomputing* 493 (2022), pp. 28–45.

[8] A. Yale, S. Dash, R. Dutta, I. Guyon, A. Pavao, and K. P. Bennett. “Generation and evaluation of privacy preserving synthetic health data”. In: *Neurocomputing* 416 (2020), pp. 244–255. ISSN: 0925-2312. DOI: https://doi.org/10.1016/j.neucom.2019.12.136. URL: https://www.sciencedirect.com/science/article/pii/S0925231220305117.

[9] K. Armanious, C. Jiang, M. Fischer, T. Küstner, T. Hepp, K. Nikolaou, S. Gatidis, and B. Yang. “MedGAN: Medical image translation using GANs”. In: *Computerized Medical Imaging and Graphics* 79 (2020), p. 101684. ISSN: 0895-6111. DOI: https://doi.org/10.1016/j.compmedimag.2019.101684. URL: https://www.sciencedirect.com/science/article/pii/S0895611119300990.

[10] L. Xu, M. Skoularidou, A. Cuesta-Infante, and K. Veeramachaneni. “Modeling tabular data using conditional gan”. In: *Advances in neural information processing systems* 32 (2019).

[11] J. P. Reiter. “Using CART to generate partially synthetic public use microdata”. In: *Journal of Official Statistics* 21 (2005), pp. 441–462. URL: https://api.semanticscholar.org/CorpusID:2977015.

[12] N. Patki, R. Wedge, and K. Veeramachaneni. “The synthetic data vault”. In: *2016 IEEE international conference on data science and advanced analytics (DSAA)*. IEEE. 2016, pp. 399–410.

[13] D. Kaur, M. Sobiesk, S. Patil, J. Liu, P. Bhagat, A. Gupta, and N. Markuzon. “Application of Bayesian networks to generate synthetic health data”. In: *Journal of the American Medical Informatics Association* 28.4 (Dec. 2020), pp. 801–811. ISSN: 1527-974X. DOI: 10.1093/jamia/ocaa303. eprint: https://academic.oup.com/jamia/article-pdf/28/4/801/36642121/ocaa303.pdf. URL: https://doi.org/10.1093/jamia/ocaa303.

[14] DNV. *The Veracity Platform*. URL: https://www.veracity.com.

[15] MIT. *The Synthetic Data Vault (SDV)*. URL: https://docs.sdv.dev/sdv.

[16] Cancer Registry of Netherland. *Synthetic Dataset*. URL: https://iknl.nl/en/ncr/synthetic-dataset.

[17] N. Patki, R. Wedge, and K. Veeramachaneni. “The Synthetic Data Vault”. In: *2016 IEEE International Conference on Data Science and Advanced Analytics (DSAA)*. 2016, pp. 399–410. DOI: 10.1109/DSAA.2016.49.

[18] MIT. *Copulas, The Synthetic Data Vault (SDV)*. URL: https://sdv.dev/Copulas/.

[19] MIT. *TVAESynthesizer. The Synthetic Data Vault (SDV)*. URL: https://docs.sdv.dev/sdv/single-table-data/modeling/synthesizers/tvaesynthesizer.

[20] MIT. *CTGANSynthesizer. The Synthetic Data Vault (SDV)*. URL: https://docs.sdv.dev/sdv/single-table-data/modeling/synthesizers/ctgansynthesizer.

[21] MIT. *GaussianCopulaSynthesizer. The Synthetic Data Vault (SDV)*. URL: https://docs.sdv.dev/sdv/single-table-data/modeling/synthesizers/gaussiancopulasynthesizer.

[22] MIT. *GaussianCopulaSynthesizer source code*. URL: https://github.com/sdv-dev/SDV/blob/main/sdv/single_table/copulas.py.

[23] MIT. *TVAESynthesizer source code*. URL: https://github.com/sdv-dev/CTGAN/blob/main/ctgan/synthesizers/tvae.py.

[24] MIT. *CTGANSynthesizer source code*. URL: https://github.com/sdv-dev/CTGAN/blob/main/ctgan/synthesizers/ctgan.py.

[25] MIT. *QulityReport documentation*. URL: https://docs.sdv.dev/sdmetrics/reports/quality-report.

[26] MIT. *QulityReport documentation*. URL: https://docs.sdv.dev/sdmetrics/reports/diagnostic-report.

[27] K. El Emam, L. Mosquera, and R. Hoptroff. *Practical synthetic data generation: balancing privacy and the broad availability of data*. O’Reilly Media, 2020.

[28] Z. Qian, B.-C. Cebere, and M. van der Schaar. “Synthcity: facilitating innovative use cases of synthetic data in different data modalities”. In: *arXiv preprint arXiv:2301.07573* (2023).

[29] F. K. Dankar, M. K. Ibrahim, and L. Ismail. “A multi-dimensional evaluation of synthetic data generators”. In: *IEEE Access* 10 (2022), pp. 11147–11158.

A Figures and images

This appendix includes larger images of the figures in the article and an additional data dictionary from the IKNL dataset.

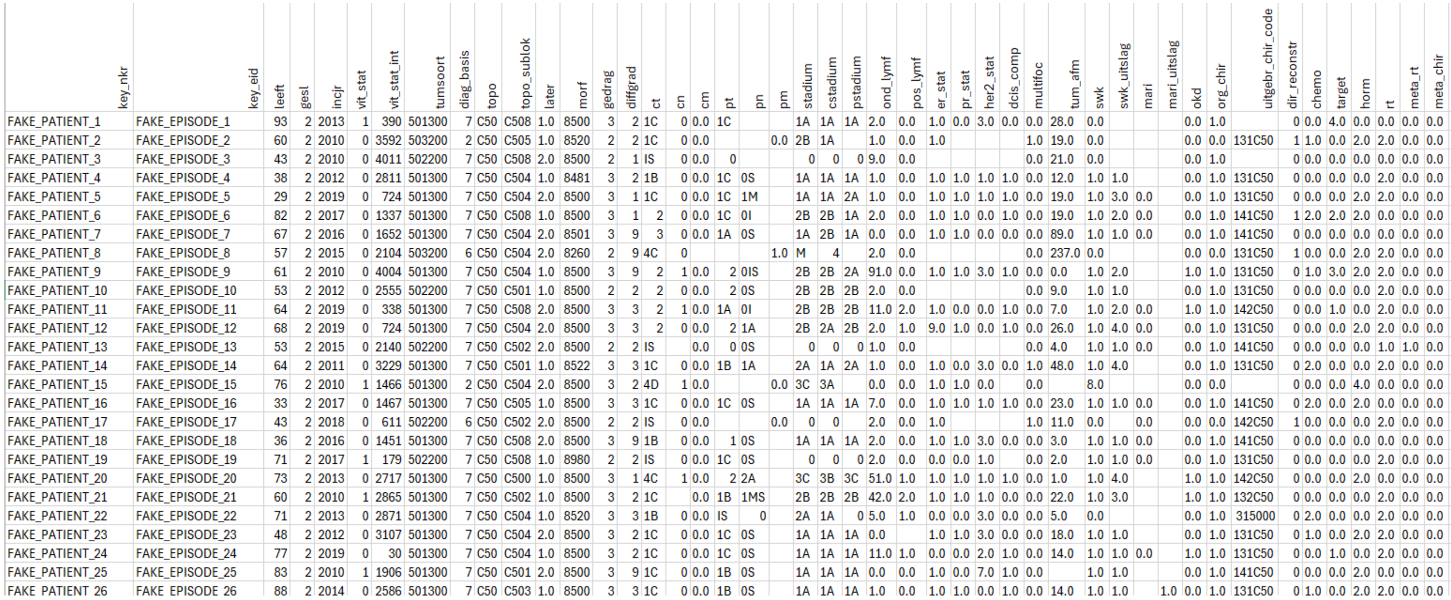

key_nkr	key_eid	leeft	gesl	incjr	vit_stat	vit_stat_int	tumsoort	diag_basis	topo	topo_sublok	later	morf	gedrag	diffgrad	ct	cn	cm	pt	pn	pm	stadium	cstadium	pstadium	ond_lymf	pos_lymf	er_stat	pr_stat	her2_stat	dcis_comp	multifoc	tum_afm	swk	swk_uitslag	mari	mari_uitslag	okd	org_chir	uitgebr_chir_code	dir_reconstr	chemo	target	horm	rt	meta_rt	meta_chir
FAKE_PATIENT_1	FAKE_EPISODE_1	93	2	2013	1	390	501300	7	C50	C508	1.0	8500	3	2	1C	0	0.0	1C			1A	1A	1A	2.0	0.0	1.0	0.0	3.0	0.0	0.0	28.0	0.0				0.0	1.0		0	0.0	4.0	0.0	0.0	0.0	0.0
FAKE_PATIENT_2	FAKE_EPISODE_2	60	2	2010	0	3592	503200	2	C50	C505	1.0	8520	2	2	1C	0	0.0			0.0	2B	1A		1.0	0.0	1.0				1.0	19.0	0.0				0.0	0.0	131C50	1	1.0	0.0	2.0	2.0	0.0	0.0
FAKE_PATIENT_3	FAKE_EPISODE_3	43	2	2010	0	4011	502200	7	C50	C508	2.0	8500	2	1	IS	0	0.0	0			0	0	0	9.0	0.0					0.0	21.0	0.0				0.0	1.0		0	0.0	0.0	0.0	0.0	0.0	0.0
FAKE_PATIENT_4	FAKE_EPISODE_4	38	2	2012	0	2811	501300	7	C50	C504	1.0	8481	3	2	1B	0	0.0	1C	0S		1A	1A	1A	1.0	0.0	1.0	1.0	1.0	1.0	0.0	12.0	1.0	1.0			0.0	1.0	131C50	0	0.0	0.0	0.0	2.0	0.0	0.0
FAKE_PATIENT_5	FAKE_EPISODE_5	29	2	2019	0	724	501300	7	C50	C504	2.0	8500	3	1	1C	0	0.0	1C	1M		1A	1A	2A	1.0	0.0	1.0	1.0	1.0	1.0	0.0	19.0	1.0	3.0	0.0		0.0	1.0	131C50	0	0.0	0.0	2.0	2.0	0.0	0.0
FAKE_PATIENT_6	FAKE_EPISODE_6	82	2	2017	0	1337	501300	7	C50	C508	1.0	8500	3	1	2	0	0.0	1C	0I		2B	2B	1A	2.0	0.0	1.0	1.0	0.0	1.0	0.0	19.0	1.0	2.0	0.0		0.0	1.0	141C50	1	2.0	2.0	2.0	0.0	0.0	0.0
FAKE_PATIENT_7	FAKE_EPISODE_7	67	2	2016	0	1652	501300	7	C50	C504	2.0	8501	3	9	3	0	0.0	1A	0S		1A	2B	1A	0.0	0.0	1.0	1.0	0.0	0.0	0.0	89.0	1.0	1.0	0.0		0.0	1.0	141C50	0	0.0	0.0	0.0	0.0	0.0	0.0
FAKE_PATIENT_8	FAKE_EPISODE_8	57	2	2015	0	2104	503200	6	C50	C504	2.0	8260	2	9	4C	0				1.0	M	4		2.0	0.0					0.0	237.0	0.0				0.0	0.0	131C50	1	0.0	0.0	2.0	2.0	0.0	0.0
FAKE_PATIENT_9	FAKE_EPISODE_9	61	2	2010	0	4004	501300	7	C50	C504	1.0	8500	3	9	2	1	0.0	2	0IS		2B	2B	2A	91.0	0.0	1.0	1.0	3.0	1.0	0.0	0.0	1.0	2.0			1.0	1.0	131C50	0	1.0	3.0	2.0	2.0	0.0	0.0
FAKE_PATIENT_10	FAKE_EPISODE_10	53	2	2012	0	2555	502200	7	C50	C501	1.0	8500	2	2	2	0	0.0	2	0S		2B	2B	2B	2.0	0.0					0.0	9.0	1.0	1.0			0.0	1.0	131C50	0	0.0	0.0	0.0	2.0	0.0	0.0
FAKE_PATIENT_11	FAKE_EPISODE_11	64	2	2019	0	338	501300	7	C50	C508	2.0	8500	3	3	2	1	0.0	1A	0I		2B	2B	2B	11.0	2.0	1.0	0.0	0.0	1.0	0.0	7.0	1.0	2.0	0.0		1.0	1.0	142C50	0	0.0	1.0	0.0	2.0	0.0	0.0
FAKE_PATIENT_12	FAKE_EPISODE_12	68	2	2019	0	724	501300	7	C50	C504	2.0	8500	3	3	2	0	0.0	2	1A		2B	2A	2B	2.0	1.0	9.0	1.0	0.0	1.0	0.0	26.0	1.0	4.0	0.0		0.0	1.0	131C50	0	0.0	0.0	2.0	2.0	0.0	0.0
FAKE_PATIENT_13	FAKE_EPISODE_13	53	2	2015	0	2140	502200	7	C50	C502	2.0	8500	2	2	IS		0.0	0	0S		0	0	0	1.0	0.0					0.0	4.0	1.0	1.0	0.0		0.0	1.0	141C50	0	0.0	0.0	0.0	1.0	1.0	0.0
FAKE_PATIENT_14	FAKE_EPISODE_14	64	2	2011	0	3229	501300	7	C50	C501	1.0	8522	3	3	1C	0	0.0	1B	1A		2A	1A	2A	1.0	0.0	1.0	0.0	3.0	0.0	1.0	48.0	1.0	4.0			0.0	1.0	131C50	0	2.0	0.0	0.0	2.0	0.0	0.0
FAKE_PATIENT_15	FAKE_EPISODE_15	76	2	2010	1	1466	501300	2	C50	C504	2.0	8500	3	2	4D	1	0.0			0.0	3C	3A		0.0	0.0	1.0	1.0	0.0		0.0		8.0				0.0	0.0		0	0.0	0.0	4.0	0.0	0.0	0.0
FAKE_PATIENT_16	FAKE_EPISODE_16	33	2	2017	0	1467	501300	7	C50	C505	1.0	8500	3	3	1C	0	0.0	1C	0S		1A	1A	1A	7.0	0.0	1.0	1.0	1.0	1.0	0.0	23.0	1.0	1.0	0.0		0.0	1.0	141C50	0	2.0	0.0	2.0	0.0	0.0	0.0
FAKE_PATIENT_17	FAKE_EPISODE_17	43	2	2018	0	611	502200	6	C50	C502	2.0	8500	2	2	IS	0	0.0			0.0	0	0		2.0	0.0	1.0				1.0	11.0	0.0		0.0		0.0	0.0	142C50	1	0.0	0.0	0.0	2.0	0.0	0.0
FAKE_PATIENT_18	FAKE_EPISODE_18	36	2	2016	0	1451	501300	7	C50	C508	2.0	8500	3	9	1B	0	0.0	1	0S		1A	1A	1A	2.0	0.0	1.0	1.0	3.0	0.0	0.0	3.0	1.0	1.0	0.0		0.0	1.0	141C50	0	0.0	0.0	0.0	0.0	0.0	0.0
FAKE_PATIENT_19	FAKE_EPISODE_19	71	2	2017	1	179	502200	7	C50	C508	1.0	8980	2	2	IS	0	0.0	1C	0S		0	0	0	2.0	0.0	0.0	0.0	1.0		0.0	2.0	1.0	1.0	0.0		0.0	1.0	131C50	0	0.0	0.0	0.0	2.0	0.0	0.0
FAKE_PATIENT_20	FAKE_EPISODE_20	73	2	2013	0	2717	501300	7	C50	C500	1.0	8500	3	1	4C	1	0.0	2	2A		3C	3B	3C	51.0	1.0	1.0	1.0	1.0	1.0	0.0	1.0	1.0	4.0			1.0	1.0	142C50	0	0.0	0.0	2.0	0.0	0.0	0.0
FAKE_PATIENT_21	FAKE_EPISODE_21	60	2	2010	1	2865	501300	7	C50	C502	1.0	8500	3	2	1C		0.0	1B	1MS		2B	2B	2B	42.0	2.0	1.0	1.0	1.0	0.0	0.0	22.0	1.0	3.0			1.0	1.0	132C50	0	0.0	0.0	0.0	2.0	0.0	0.0
FAKE_PATIENT_22	FAKE_EPISODE_22	71	2	2013	0	2871	501300	7	C50	C504	1.0	8520	3	3	1B	0	0.0	IS	0		2A	1A	0	5.0	1.0	0.0	0.0	3.0	0.0	0.0	5.0	0.0				0.0	1.0	315000	0	2.0	0.0	0.0	2.0	0.0	0.0
FAKE_PATIENT_23	FAKE_EPISODE_23	48	2	2012	0	3107	501300	7	C50	C504	2.0	8500	3	2	1C	0	0.0	1C	0S		1A	1A	1A	0.0		1.0	1.0	3.0	0.0	0.0	18.0	1.0	1.0			0.0	1.0	131C50	0	1.0	0.0	2.0	2.0	0.0	0.0
FAKE_PATIENT_24	FAKE_EPISODE_24	77	2	2019	0	30	501300	7	C50	C504	1.0	8500	3	2	1C	0	0.0	1C	0S		1A	1A	1A	11.0	1.0	0.0	0.0	2.0	1.0	0.0	14.0	1.0	1.0	0.0		1.0	1.0	131C50	0	0.0	1.0	0.0	2.0	0.0	0.0
FAKE_PATIENT_25	FAKE_EPISODE_25	83	2	2010	1	1906	501300	7	C50	C501	2.0	8500	3	9	1C	0	0.0	1B	0S		1A	1A	1A	0.0	0.0	1.0	0.0	7.0	1.0	0.0		1.0	1.0			0.0	1.0	141C50	0	0.0	0.0	2.0	0.0	0.0	0.0
FAKE_PATIENT_26	FAKE_EPISODE_26	88	2	2014	0	2586	501300	7	C50	C503	1.0	8500	3	3	1C	0	0.0	1B	0S		1A	1A	1A	1.0	0.0	1.0	1.0	0.0	1.0	0.0	14.0	1.0	1.0		1.0	0.0	1.0	131C50	0	1.0	0.0	2.0	2.0	0.0	0.0

Figure A.1. Snip of the raw data from the IKNL dataset

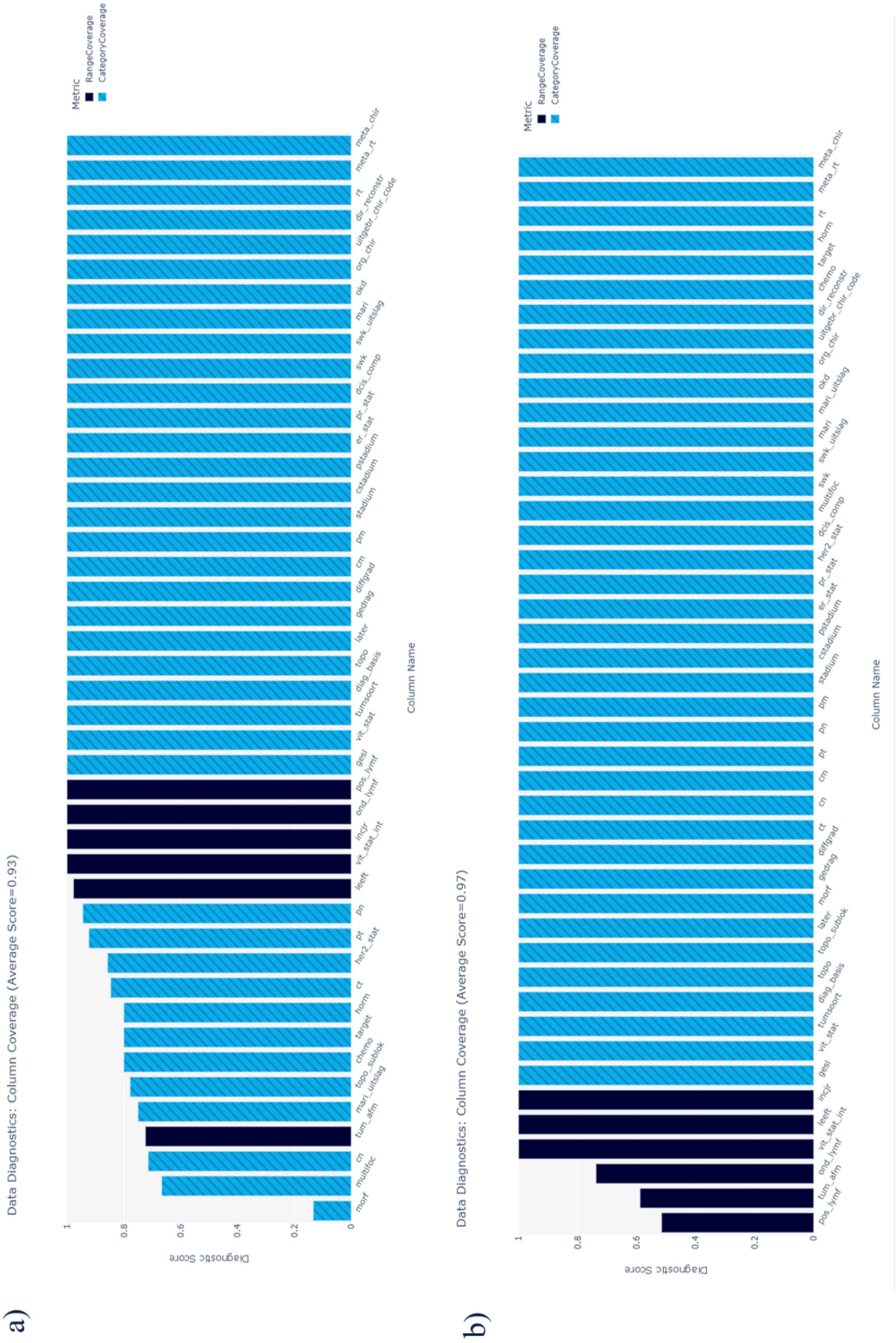

Figure A.2. Detailing of the average column coverage score when the meta data was defined, comparing a) TVAE results and b) GaussianCopula results. The dark blue RangeCoverage is for numerical values and the light blue CategoryCoverage is for categorical data.

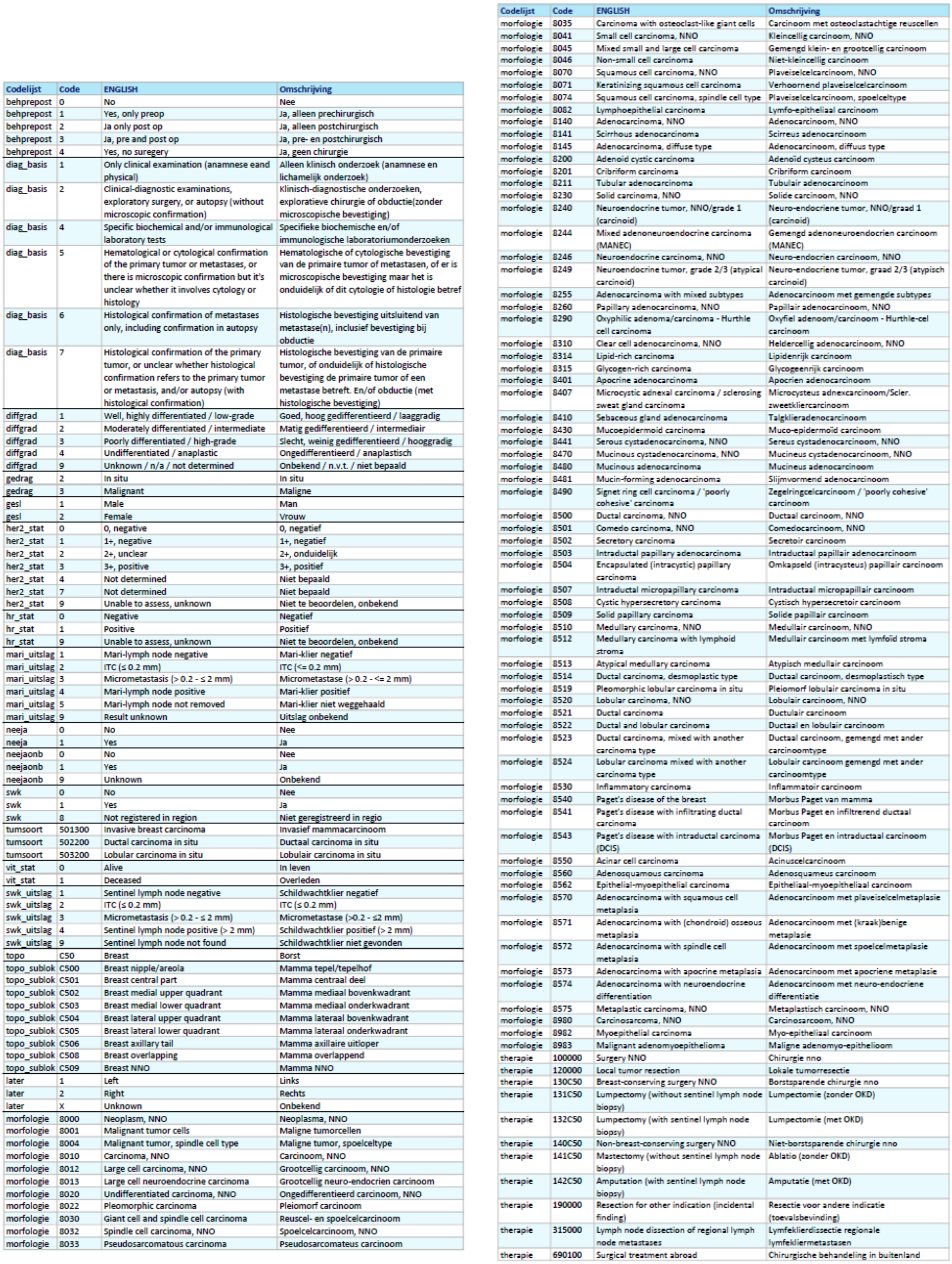

Codelijst	Code	ENGLISH	Omschrijving
behprepost	0	No	Nee
behprepost	1	Yes, only preop	Ja, alleen prechirurgisch
behprepost	2	Ja only post op	Ja, alleen postchirurgisch
behprepost	3	Ja, pre and post op	Ja, pre- en postchirurgisch
behprepost	4	Yes, no suregery	Ja, geen chirurgie
diag_basis	1	Only clinical examination (anamnese eand physical)	Alleen klinisch onderzoek (anamnese en lichamelijk onderzoek)
diag_basis	2	Clinical-diagnostic examinations, exploratory surgery, or autopsy (without microscopic confirmation)	Klinisch-diagnostische onderzoeken, explorative chirurgie of obductie(zonder microscopische bevestiging)
diag_basis	4	Specific biochemical and/or immunological laboratory tests	Specifieke biochemische en/of immunologische laboratoriumonderzoeken
diag_basis	5	Hematological or cytological confirmation of the primary tumor or metastases, or there is microscopic confirmation but it's unclear whether it involves cytology or histology	Hematologische of cytologische bevestiging van de primaire tumor of metastasen, of er is microscopische bevestiging maar het is onduidelijk of dit cytologie of histologie betref
diag_basis	6	Histological confirmation of metastases only, including confirmation in autopsy	Histologische bevestiging uitsluitend van metastase(n), inclusief bevestiging bij obductie
diag_basis	7	Histological confirmation of the primary tumor, or unclear whether histological confirmation refers to the primary tumor or metastasis, and/or autopsy (with histological confirmation)	Histologische bevestiging van de primaire tumor, of onduidelijk of histologische bevestiging de primaire tumor of een metastase betreft. En/of obductie (met histologische bevestiging)
diffgrad	1	Well, highly differentiated / low-grade	Goed, hoog gedifferentieerd / laaggradig
diffgrad	2	Moderately differentiated / intermediate	Matig gedifferentieerd / intermediair
diffgrad	3	Poorly differentiated / high-grade	Slecht, weinig gedifferentieerd / hooggradig
diffgrad	4	Undifferentiated / anaplastic	Ongedifferentieerd / anaplastisch
diffgrad	9	Unknown / n/a / not determined	Onbekend / n.v.t. / niet bepaald
gedrag	2	In situ	In situ
gedrag	3	Malignant	Maligne
gesl	1	Male	Man
gesl	2	Female	Vrouw
her2_stat	0	0, negative	0, negatief
her2_stat	1	1+, negative	1+, negatief
her2_stat	2	2+, unclear	2+, onduidelijk
her2_stat	3	3+, positive	3+, positief
her2_stat	4	Not determined	Niet bepaald
her2_stat	7	Not determined	Niet bepaald
her2_stat	9	Unable to assess, unknown	Niet te beoordelen, onbekend
hr_stat	0	Negative	Negatief
hr_stat	1	Positive	Positief
hr_stat	9	Unable to assess, unknown	Niet te beoordelen, onbekend
mari_uitslag	1	Mari-lymph node negative	Mari-klier negatief
mari_uitslag	2	ITC (≤ 0.2 mm)	ITC (<= 0.2 mm)
mari_uitslag	3	Micrometastasis (> 0.2 - ≤ 2 mm)	Micrometastase (> 0.2 - <= 2 mm)
mari_uitslag	4	Mari-lymph node positive	Mari-klier positief
mari_uitslag	5	Mari-lymph node not removed	Mari-klier niet weggehaald
mari_uitslag	9	Result unknown	Uitslag onbekend
neeja	0	No	Nee
neeja	1	Yes	Ja
neejaonb	0	No	Nee
neejaonb	1	Yes	Ja
neejaonb	9	Unknown	Onbekend
swk	0	No	Nee
swk	1	Yes	Ja
swk	8	Not registered in region	Niet geregistreerd in regio
tumsoort	501300	Invasive breast carcinoma	Invasief mammacarcinoom
tumsoort	502200	Ductal carcinoma in situ	Ductaal carcinoma in situ
tumsoort	503200	Lobular carcinoma in situ	Lobulair carcinoma in situ
vit_stat	0	Alive	In leven
vit_stat	1	Deceased	Overleden
swk_uitslag	1	Sentinel lymph node negative	Schildwachtklier negatief
swk_uitslag	2	ITC (≤ 0.2 mm)	ITC (≤ 0.2 mm)
swk_uitslag	3	Micrometastasis (> 0.2 - ≤ 2 mm)	Micrometastase (>0.2 - ≤2 mm)
swk_uitslag	4	Sentinel lymph node positive (> 2 mm)	Schildwachtklier positief (> 2 mm)
swk_uitslag	9	Sentinel lymph node not found	Schildwachtklier niet gevonden
topo	C50	Breast	Borst
topo_sublok	C500	Breast nipple/areola	Mamma tepel/tepelhof
topo_sublok	C501	Breast central part	Mamma centraal deel
topo_sublok	C502	Breast medial upper quadrant	Mamma mediaal bovenkwadrant
topo_sublok	C503	Breast medial lower quadrant	Mamma mediaal onderkwadrant
topo_sublok	C504	Breast lateral upper quadrant	Mamma lateraal bovenkwadrant
topo_sublok	C505	Breast lateral lower quadrant	Mamma lateraal onderkwadrant
topo_sublok	C506	Breast axillary tail	Mamma axillaire uitloper
topo_sublok	C508	Breast overlapping	Mamma overlappend
topo_sublok	C509	Breast NNO	Mamma NNO
later	1	Left	Links
later	2	Right	Rechts
later	X	Unknown	Onbekend
morfologie	8000	Neoplasm, NNO	Neoplasma, NNO
morfologie	8001	Malignant tumor cells	Maligne tumorcellen
morfologie	8004	Malignant tumor, spindle cell type	Maligne tumor, spoelceltype
morfologie	8010	Carcinoma, NNO	Carcinoom, NNO
morfologie	8012	Large cell carcinoma, NNO	Grootcellig carcinoom, NNO
morfologie	8013	Large cell neuroendocrine carcinoma	Grootcellig neuro-endocrien carcinoom
morfologie	8020	Undifferentiated carcinoma, NNO	Ongedifferentieerd carcinoom, NNO
morfologie	8022	Pleomorphic carcinoma	Pleiomorf carcinoom
morfologie	8030	Giant cell and spindle cell carcinoma	Reuscel- en spoelcelcarcinoom
morfologie	8032	Spindle cell carcinoma, NNO	Spoelcelcarcinoom, NNO
morfologie	8033	Pseudosarcomatous carcinoma	Pseudosarcomateus carcinoom
morfologie	8035	Carcinoma with osteoclast-like giant cells	Carcinoom met osteoclastachtige reuscellen
morfologie	8041	Small cell carcinoma, NNO	Kleincellig carcinoom, NNO
morfologie	8045	Mixed small and large cell carcinoma	Gemengd klein- en grootcellig carcinoom
morfologie	8046	Non-small cell carcinoma	Niet-kleincellig carcinoom
morfologie	8070	Squamous cell carcinoma, NNO	Plaveiselcelcarcinoom, NNO
morfologie	8071	Keratinizing squamous cell carcinoma	Verhoornend plaveiselcelcarcinoom
morfologie	8074	Squamous cell carcinoma, spindle cell type	Plaveiselcelcarcinoom, spoelceltype
morfologie	8082	Lymphoepithelial carcinoma	Lymfo-epitheliaal carcinoom
morfologie	8140	Adenocarcinoma, NNO	Adenocarcinoom, NNO
morfologie	8141	Scirrhous adenocarcinoma	Scirreus adenocarcinoom
morfologie	8145	Adenocarcinoma, diffuse type	Adenocarcinoom, diffuus type
morfologie	8200	Adenoid cystic carcinoma	Adenoïd cysteus carcinoom
morfologie	8201	Cribriform carcinoma	Cribriform carcinoom
morfologie	8211	Tubular adenocarcinoma	Tubulair adenocarcinoom
morfologie	8230	Solid carcinoma, NNO	Solide carcinoom, NNO
morfologie	8240	Neuroendocrine tumor, NNO/grade 1 (carcinoid)	Neuro-endocriene tumor, NNO/graad 1 (carcinoid)
morfologie	8244	Mixed adenoneuroendocrine carcinoma (MANEC)	Gemengd adenoneuroendocrien carcinoom (MANEC)
morfologie	8246	Neuroendocrine carcinoma, NNO	Neuro-endocrien carcinoom, NNO
morfologie	8249	Neuroendocrine tumor, grade 2/3 (atypical carcinoid)	Neuro-endocriene tumor, graad 2/3 (atypisch carcinoid)
morfologie	8255	Adenocarcinoma with mixed subtypes	Adenocarcinoom met gemengde subtypes
morfologie	8260	Papillary adenocarcinoma, NNO	Papillair adenocarcinoom, NNO
morfologie	8290	Oxyphilic adenoma/carcinoma - Hurthle cell carcinoma	Oxyfiel adenoom/carcinoom - Hurthle-cel carcinoom
morfologie	8310	Clear cell adenocarcinoma, NNO	Heldercellig adenocarcinoom, NNO
morfologie	8314	Lipid-rich carcinoma	Lipidenrijk carcinoom
morfologie	8315	Glycogen-rich carcinoma	Glycogeenrijk carcinoom
morfologie	8401	Apocrine adenocarcinoma	Apocrien adenocarcinoom
morfologie	8407	Microcystic adnexal carcinoma / sclerosing sweat gland carcinoma	Microcysteus adnexcarcinoom/Scler. zweetkliercarcinoom
morfologie	8410	Sebaceous gland adenocarcinoma	Talgklieradenocarcinoom
morfologie	8430	Mucoepidermoid carcinoma	Muco-epidermoïd carcinoom
morfologie	8441	Serous cystadenocarcinoma, NNO	Sereus cystadenocarcinoom, NNO
morfologie	8470	Mucinous cystadenocarcinoma, NNO	Mucineus cystadenocarcinoom, NNO
morfologie	8480	Mucinous adenocarcinoma	Mucineus adenocarcinoom
morfologie	8481	Mucin-forming adenocarcinoma	Slijmvormend adenocarcinoom
morfologie	8490	Signet ring cell carcinoma / 'poorly cohesive' carcinoma	Zegelringcelcarcinoom / 'poorly cohesive' carcinoom
morfologie	8500	Ductal carcinoma, NNO	Ductaal carcinoom, NNO
morfologie	8501	Comedo carcinoma, NNO	Comedocarcinoom, NNO
morfologie	8502	Secretory carcinoma	Secretoir carcinoom
morfologie	8503	Intraductal papillary adenocarcinoma	Intraductaal papillair adenocarcinoom
morfologie	8504	Encapsulated (intracystic) papillary carcinoma	Omkapseld (intracysteus) papillair carcinoom
morfologie	8507	Intraductal micropapillary carcinoma	Intraductaal micropapillair carcinoom
morfologie	8508	Cystic hypersecretory carcinoma	Cystisch hypersecretoir carcinoom
morfologie	8509	Solid papillary carcinoma	Solide papillair carcinoom
morfologie	8510	Medullary carcinoma, NNO	Medullair carcinoom, NNO
morfologie	8512	Medullary carcinoma with lymphoid stroma	Medullair carcinoom met lymfoïd stroma
morfologie	8513	Atypical medullary carcinoma	Atypisch medullair carcinoom
morfologie	8514	Ductal carcinoma, desmoplastic type	Ductaal carcinoom, desmoplastisch type
morfologie	8519	Pleomorphic lobular carcinoma in situ	Pleiomorf lobulair carcinoma in situ
morfologie	8520	Lobular carcinoma, NNO	Lobulair carcinoom, NNO
morfologie	8521	Ductal carcinoma	Ductulair carcinoom
morfologie	8522	Ductal and lobular carcinoma	Ductaal en lobulair carcinoom
morfologie	8523	Ductal carcinoma, mixed with another carcinoma type	Ductaal carcinoom, gemengd met ander carcinoomtype
morfologie	8524	Lobular carcinoma mixed with another carcinoma type	Lobulair carcinoom gemengd met ander carcinoomtype
morfologie	8530	Inflammatory carcinoma	Inflammatoir carcinoom
morfologie	8540	Paget's disease of the breast	Morbus Paget van mamma
morfologie	8541	Paget's disease with infiltrating ductal carcinoma	Morbus Paget en infiltrerend ductaal carcinoom
morfologie	8543	Paget's disease with intraductal carcinoma (DCIS)	Morbus Paget en intraductaal carcinoom (DCIS)
morfologie	8550	Acinar cell carcinoma	Acinuscelcarcinoom
morfologie	8560	Adenosquamous carcinoma	Adenosquameus carcinoom
morfologie	8562	Epithelial-myoepithelial carcinoma	Epitheliaal-myoepitheliaal carcinoom
morfologie	8570	Adenocarcinoma with squamous cell metaplasia	Adenocarcinoom met plaveiselcelmetaplasie
morfologie	8571	Adenocarcinoma with (chondroid) osseous metaplasia	Adenocarcinoom met (kraak)benige metaplasie
morfologie	8572	Adenocarcinoma with spindle cell metaplasia	Adenocarcinoom met spoelcelmetaplasie
morfologie	8573	Adenocarcinoma with apocrine metaplasia	Adenocarcinoom met apocriene metaplasie
morfologie	8574	Adenocarcinoma with neuroendocrine differentiation	Adenocarcinoom met neuro-endocriene differentiatie
morfologie	8575	Metaplastic carcinoma, NNO	Metaplastisch carcinoom, NNO
morfologie	8980	Carcinosarcoma, NNO	Carcinosarcoom, NNO
morfologie	8982	Myoepithelial carcinoma	Myo-epitheliaal carcinoom
morfologie	8983	Malignant adenomyoepithelioma	Maligne adenomyo-epithelioom
therapie	100000	Surgery NNO	Chirurgie nno
therapie	120000	Local tumor resection	Lokale tumorresectie
therapie	130C50	Breast-conserving surgery NNO	Borstsparende chirurgie nno
therapie	131C50	Lumpectomy (without sentinel lymph node biopsy)	Lumpectomie (zonder OKD)
therapie	132C50	Lumpectomy (with sentinel lymph node biopsy)	Lumpectomie (met OKD)
therapie	140C50	Non-breast-conserving surgery NNO	Niet-borstsparende chirurgie nno
therapie	141C50	Mastectomy (without sentinel lymph node biopsy)	Ablatio (zonder OKD)
therapie	142C50	Amputation (with sentinel lymph node biopsy)	Amputatie (met OKD)
therapie	190000	Resection for other indication (incidental finding)	Resectie voor andere indicatie (toevalsbevinding)
therapie	315000	Lymph node dissection of regional lymph node metastases	Lymfeklierdissectie regionale lymfekliermetastasen
therapie	690100	Surgical treatment abroad	Chirurgische behandeling in buitenland

Figure A.3. Data dictionary - labels from the IKNL dataset. The complete dictionary is available at the website of the Cancer Registry of Netherland ([16]).

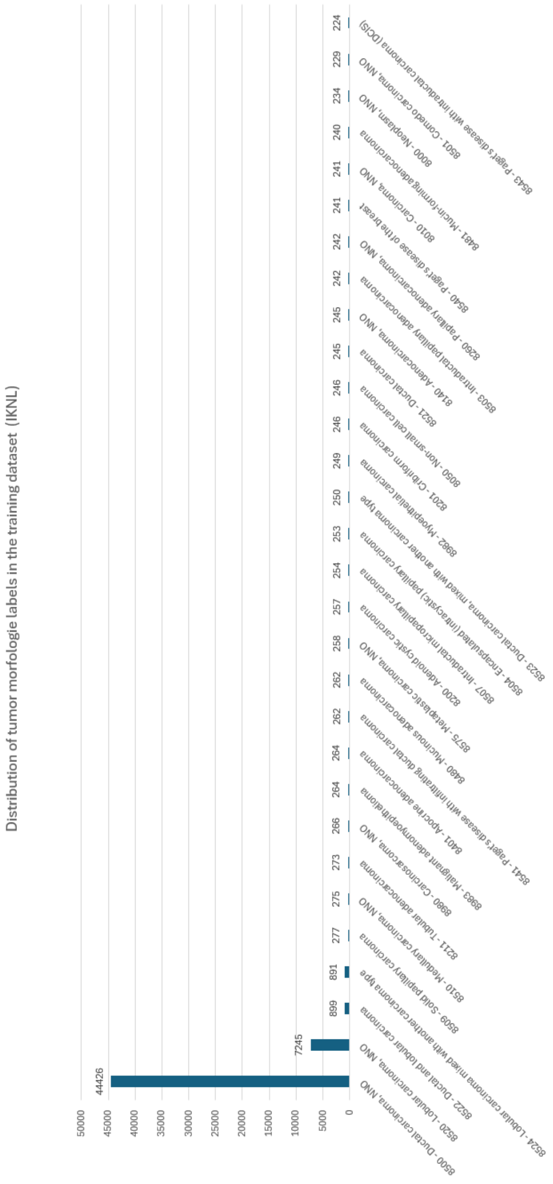

Figure A.4. Distribution of tumor morphology in the IKNL dataset (the training dataset for this experiment).